Cassini Cosmic Dust Analyser: Composition of dust at Saturn

Book Section

CASSINI COSMIC DUST ANALYSER: COMPOSITION OF DUST AT SATURN

N. McBride[(1)], J.K. Hillier[(1)], S.F. Green[(1)], R. Srama[(2)], S. Kempf[(2)], F. Postberg[(2)], G. Moragas-Klostermeyer[(2)], J.A.M. McDonnell[(1)], E. Grün[(2,3)]

[(1)]Planetary and Space Sciences Research Institute, The Open University, Walton Hall, Milton Keynes, MK76AA, UK, Email: n.m.mcbride@open.ac.uk.
[(2)]MPI für Kernphysik, Saupfercheckweg 1, 69117 Heidelberg, Germany.
[(3)]Hawaii Institute of Geophysics and Planetology, University of Hawaii, 1680 East West Road, POST 512c, Honolulu, Hawaii, HI 96822, USA.

ABSTRACT

We discuss issues involved with interpreting time-of-flight mass spectra (TOFMS) obtained by the Chemical Analyser subsystem of the Cassini Cosmic Dust Analyser (CDA). We use an in-house ion dynamics code specifically written for CDA which helps us to understand and constrain the initial impact plasma ion kinetic energy and angular distributions. We also present some typical results obtained from within the Saturnian system. We find that particles predominantly consist of water ice (manifesting itself in the TOFMS as hydronium ions, with varying numbers of water molecules attached) and minor silicate impurities. Some ammonia may also be present.

1. INTRODUCTION

The Cosmic Dust Analyser (CDA) [1] aboard the Cassini spacecraft has been sampling dust within the Saturnian system since orbit insertion in July 2004. CDA consists of two primary subsystems: the Dust Analyser subsystem, with instruments capable of measuring charge, velocity, mass, low-rate flux and the composition of dust particles, and the High-Rate Detector (HRD) which measures high-rate fluxes of impacting particles using a PVDF impact sensing system. The Dust Analyser uses the characteristics of the plasma generated by an impact of a dust particle on a metal target to determine (approximately) particle mass and speed. A crucial subsystem of CDA is the Chemical Analyser, which produces positive ion time-of-flight mass spectra (TOFMS) so obtaining some in-situ elemental and chemical information about the impacting dust. The Chemical Analyser is now returning thousands of spectra from the Saturnian system. For example, during a single ring plane crossing (the descending ring plane crossing in October 2004), it produced nearly 300 TOFMS of E ring dust particles at a distance of ~$8R_S$ from Saturn. This short paper discusses some of the issues involved with interpreting the spectra, briefly describes an ion dynamics code written specifically for CDA, and presents some typical results obtained from within the Saturnian system.

2. INTERPRETING SPECTRA

The Chemical Analyser uses a discrete central rhodium target section within the Dust Analyser (Figure 1). This target is held at +1000 V with respect to a mesh grid (0 V) 3 mm in front of it, producing a strong electric field that accelerates impact-generated cations towards focus grids (-350 V) and an electron multiplier (-2750 V), so producing the cation TOFMS. Interpreting these TOFMS can be complicated. In principle the arrival time at the multiplier, of an initially stationary ion, is governed by the relation $t = b + a\sqrt{m}$, where m is the ion mass, b is a zero point time offset, and a is a 'stretch' parameter related to the instrument geometry and field strength. However, this behaviour is complicated by the initial speed and angular distribution of the ions, any plasma shielding effects, differing geometries within the instrument, and unknown zero-point offsets attributable to triggering time differences.

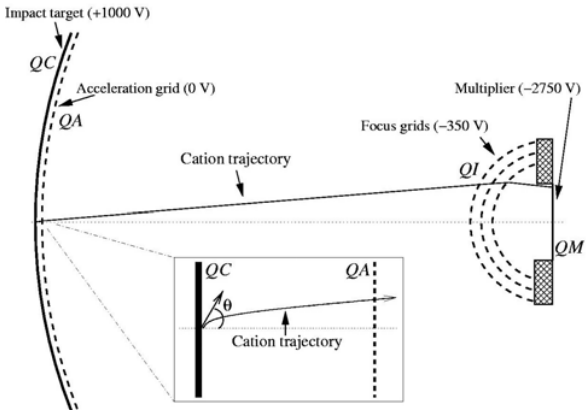

Figure 1. Schematic of the Chemical Analyser, showing the spherical section rhodium target (left) and the multiplier (right). Electrons detected on the target give a charge signal QC, and ion signals QA, QI and QM are obtained from ions impacting the accelerating mesh, the multiplier focus grids, and the multiplier respectively (QM being the actual spectrum signal). The initial ion emission angle is defined by θ. The cation trajectory shows the case where an ion is 'just detected'.

Proc. 'Dust in Planetary Systems', Kauai, Hawaii, USA. 26--30 September 2005 (ESA SP-643, January 2007)

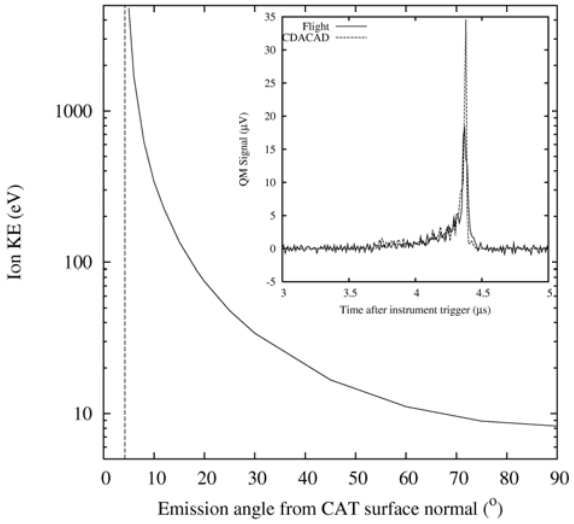

Figure 2. The maximum initial kinetic energy that an ion can have and still be detected by the Chemical Analyser multiplier as a function of the ion emission angle from the CAT surface. The inset shows a rhodium peak from a fast in situ impact (CDACAD fit also shown). The peak shape reflects the detector energy-angle response fuction.

In cases where the ion species corresponding to at least two peaks in a spectrum can be identified unambiguously, the *a* and *b* parameters can be determined with reasonable accuracy. However the aforementioned effects mean that a given ion species (a single *m* value) will give rise to spectral peaks which can vary from very narrow to extremely broad. Furthermore, the peak width and overall peak shape is likely to depend also on the impact velocity, mass and composition of the dust particle. Identification of mass species within the TOFMS, and interpretation of peak shapes can be made easier by understanding the ion dynamics within the instrument as a whole. To this end, an in-house ion dynamics code (CDACAD) was written specifically for the CDA instrument [2]. The code can treat many ion species within the whole CDA instrument, and offers a more user friendly approach than modeling individual regions of the instrument in (for example) Simion 3D software. The code releases a distribution of ions from any desired point on the Chemical Analyser target (CAT), with the ions having a user-defined initial kinetic energy distribution, and an initial trajectory direction distribution. This direction distribution is essentially a distribution of the ion emission angles θ (see Figure 1) as axial symmetry around the surface normal is usually assumed. Whether an individual ion with an initial energy and emission angle reaches the multiplier depends on the geometry and electric fields within CDA. Figure 2 shows the maximum initial kinetic energy that an ion can have and still be detected by the multiplier, as a function of the ion emission angle. It is seen that for θ <4.2º all ions are detected at the multiplier regardless of ion energy, however, as emission angles increase, increasingly more ions 'miss' the multiplier and impact other structures or are lost from the instrument altogether. Although, all ions with energies <8.3 eV will be detected regardless of emission angle. Given a broad initial energy distribution of ions, the peak shape observed in a spectrum is essentially a result of this energy versus angle 'response function'. This is demonstrated by the inset in Figure 2 which shows a rhodium peak (i.e. target material) produced by a fast (~100 km s^{-1}) in situ 'stream particle' impact (see e.g. [3]). The model fit is produced by a simplest-case uniform energy distribution and isotropic angular emission of ions. The peak shape reflects the instrument response function. Some subtleties are worthy of comment. 1) One cannot assume that ions arriving at a specific time had a specific initial energy, as many ion trajectories will result in the same arrival time depending on the emission angle of the individual ions. 2) One cannot assume that the peak is due to ions emitted with 0 eV initial energy (although typically all peaks will be dominated by ions with energy <20 eV). 3) The last ions to reach the multiplier (i.e. defining the right hand edge of the spectral feature) are not 0 eV ions, but are moderate energy ions (up to ~10 eV) released at high emission angles. 4) The leftmost edge of the spectral feature is due to the subset of highest energy ions released with θ <4.2º. Because the peak shape is so affected by the instrument angular response function, precise (and unique) combinations of ion angular and energy distributions cannot be derived from a spectral peak. However broad constraints can be produced. For example, the extended left hand flanks of the fast-impact feature shown in the Figure 2 inset requires ions with initial energies up to ~400 eV (although the main peak is dominated by ions of <20 eV). Indeed, even with low velocity (<10 km s^{-1}) impacts (see below), ions can have energies of up to ~100 eV (although the main peak is again dominated by ions of <20 eV). This is perhaps surprising considering some laboratory studies have reported low ion energies, but is consistent with work such as [4, 5]. Indeed rather than a uniform energy distribution, better fits are obtained with low energy ions being depleted and a peak at moderate energies i.e. a Gaussian with a superimposed high energy tail, or a broad Maxwell-Boltzmann distribution, fit well. While the precise ion angular distribution cannot be derived, it is clear (particularly from the rightmost flank of the spectral features i.e. the last ions to reach the multiplier) that a very broad angular emission distribution exists. Indeed, all our model fits are adequately satisfied by a

simple isotropic emission from the impact site, and certainly a narrow emission function (such as e.g. $\cos^3 \theta$) is ruled out. Finally, the high ion energies (several tens of eV) seen to dominate the in-situ spectra, and the existence of many molecular clusters (see below) means that the impact plasma (at the time ions are removed and accelerated to the multiplier) is almost certainly not in local thermal equilibrium, as the implied temperatures would have to be excessively high (10^5-10^6 K).

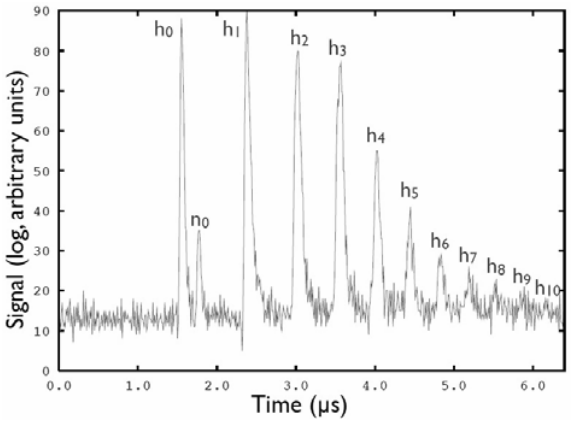

Figure 3. A particle spectra from the March 9 2005 crossing of the E ring plane. The repetitive h features show water molecular clusters (see text).

3. SPECTRA AT SATURN

Many thousands of spectra will be accumulated during Cassini's tour of the Saturnian system. To date, many fast stream particles [6] have been identified, but the majority of spectra at Saturn have come from ring particles on Keplerian orbits within the ring plane (with relative impact velocities typically between 5 and 10 km s^{-1}) (see [7]). Of these, many spectra have relatively clean, well defined 'narrow' peaks, however many also have 'wide' peaks which appear to be from particles of identical (or similar) composition, but which are more massive. The widening of the peaks is thought to be due to collisions and shielding effects in the plasma [7]. We present here two 'narrow' type spectra from the March 9 2005 E ring plane crossing (plotted logarithmically to bring out low level detail). Figure 3 shows a particularly 'clean' spectrum with a composition representative of the majority of E-ring particles. The spectrum has no strong hydrogen peak (for triggering reasons) or a discernable target (rhodium) peak. This makes determining masses more difficult, but underlines the importance of the modelling work for giving confidence to interpretations. Figure 3 is in fact due to water ice. The first major peak labelled h_0 is due to hydronium (H_3O^+) ions. The other h peaks are due to H_3O^+ ions clustering with increasing numbers of H_2O molecules i.e. h_j (j=0–10) indicates $(H_20)_jH_3O^+$. The n_0 peak is due to Na^+ ions (sodium is a target surface contaminant). The water-derived repetitive features are similar to those seen in laboratory-based experiments with organic particles [8] and impacts onto water ice [9] and are attributed to molecular cluster ions. Figure 4 shows another spectrum, again showing the h_j water-ion clusters, but also with other species too. Sodium (n_0) is again present, but now Na-water clusters are observed i.e. n_j (j=0–2) indicate $(H_20)_jNa^+$ and/or $Na(H_20)_{j-1}H_3O^+$ (j>0). r_j (j = 0–5) indicates target-water clusters i.e. $(H_2O)_jRh^+$ and/or $Rh(H_20)_{j-1}H_3O^+$ (j>0). c is C^+. s_0 is Si^+; s_1 is SiO^+ or SiH_3O^+. y_0 is H^+ with y_1 and y_2 appearing to be HH^+ and H_2H+ clusters respectively. Peak 'a' is probably NH_4^+. As stated above, the interpretation of the ion species is made easier by recourse to the CDACAD model. As an example, Figure 5 shows a spectrum (plotted linearly to show the true peak shapes) with a full model fit. The ion angular distribution was isotropic, and the energy distribution used was Maxwell-Boltzmann (modal value ~25 eV and extending to around 80 eV).

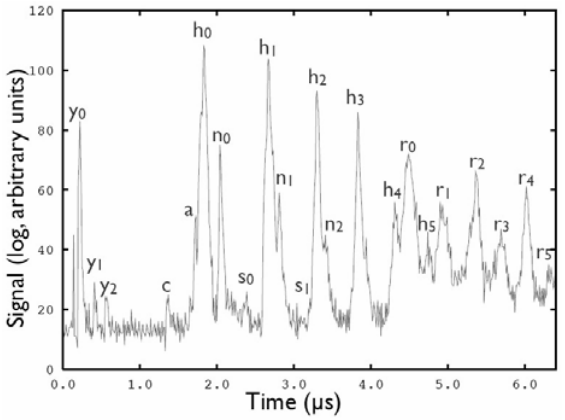

Figure 4. A particle spectra from the March 9 2005 crossing of the E ring plane. The repetitive h features show water as in Figure 3, but other species are also present including target-ion clusters (see text).

4. DISCUSSION

The Chemical Analyser data represent the first direct detection of water ice particles in Saturn's dusty E-ring. While the presence of water ice in the main 'icy' rings (A, B and C) has long been known via reflectance spectroscopy (see e.g. [10]), the 'dusty' rings (E and G) are faint with low optical depths which makes obtaining reflectance spectra extremely difficult. Consequently, until now, the composition of dusty ring particles has only been inferred from the slope of broadband photometric measurements [11] (which are in fact more sensitive to particle size distributions than composition), and the assumed link with the main rings and possible source moons. The unambiguous detection of water ice

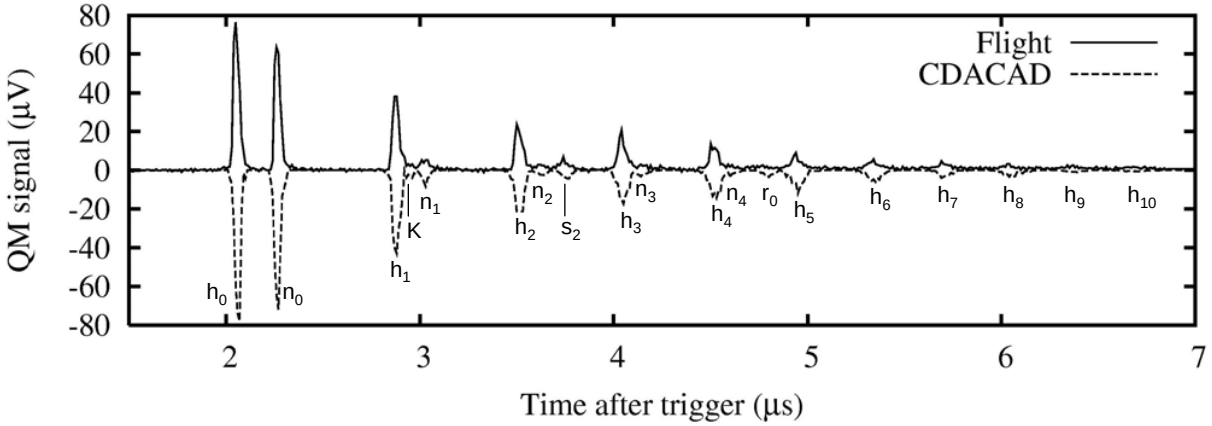

Figure 5. A particle flight spectra from a crossing of the E ring plane (plotted linearly to show the true peak shapes). The modelled fit using CDACAD is also shown, inverted (for clarity). The species used are identified as with Figures 3 and 4 (plus K denoting potassium which, like Na, is a surface contaminant, and s_2 is $SiOH_30^+$ or $SiOH_20^+$).

is thus an important result. As well as water, small amounts of silicon materials are detected. Si has already been seen [3] before orbit insertion, in stream particles emanating from the E-ring [6]. Small amounts of ammonia are also present. This is interesting as E ring particles are now thought to be primarily from localised emission from Enceladus via cryovolcanic processes [12, 13]. While remote sensing shows that there is little ammonia (or silicate material) on a large scale across Enceladus, material from localised warmer cryovolcanic regions may indeed be consistent with higher concentrations of volatile compounds. As the impurities (i.e. not water) substances in the Chemical Analyser spectra account for no more than 1% of the collected ions (i.e. below the threshold for much of the remote sensing detections), the ongoing accumulation of spectra, and correlation with specific spatial regions, is likely to offer the best opportunity to probe the composition of discrete dust particles emitted from Enceladus.

Acknowledgement: This research was supported by the Particle Physics and Astronomy Research Council.

5. REFERENCES

[1] Srama, R. *et al*. The Cassini cosmic dust analyser. *Space Sci. Rev*. **114**, 465-518 (2004).

[2] Hillier, J.K., McBride, N., Green, S.F., Kempf, S., Srama, S. Modelling CDA mass spectra. *Planet. Space Sci*., submitted.

[3] Kempf, S. *et al*. Composition of saturnian stream particles. *Science,* **307**, 1274-1276 (2005).

[4] Ratcliff, P.R., Burchell, M.J., Cole, M.J., Murphy, T.W., Alladfadi, F. Experimental measurements of hypervelocity impact plasma yield and energetics. *Int. J. Impact Engng.*, **20**, 663-674, 1997.

[5] Ratcliff, A., Allahdadi, F. Characteristics of the plasma from a 94 km s^{-1} micro-particle impact. *Adv. Space Res*., **17**, 87-91 (1996).

[6] Kempf, S. *et al*. High-velocity streams of dust originating from Saturn. *Nature,* **433**, 289-291 (2005).

[7] Hillier, J.K., Green, S.F., McBride, N., Schwanethal, J.P., Srama, R., Kempf, S., Postberg, F., Moragas-Klostermeyer, G., McDonnell, J.A.M., Grün, E. The composition of Saturn's E ring. *Mon. Not. R. astr. Soc*., in prep.

[8] Goldsworthy, B.J. *et al*. Time of flight mass spectra of ions in plasmas produced by hypervelocity impacts of organic and mineralogical microparticles on a cosmic dust analyser. *Astron. & Astrophys.,* **409**, 1151-1167 (2003).

[9] Timmermann, T., Grün, E. Plasma emission from high velocity impacts of microparticles onto water ice. *Origin and Evolution of Interplanetary Dust.* Kluwer, Dordrecht. 387-438, (1991).

[10] Poulet, F., Cruikshank, D.P., Cuzzi, J.N., Roush, T.L., French, R.G. Compositions of Saturn's rings A, B, and C from high resolution near-infrared spectroscopic observations. *Astron. Astrophys.*, **412**, 305-316 (2003).

[11] Nicholson, P.D. *et al.* Observations of Saturn's ring-plane crossings in August and November 1995. *Science,* **272**, 509-515 (1996).

[12] Press release from the Cassini project team, see http://Saturn.jpl.nasa.gov/multimedia/images/image-details.cfm?imageID=1691

[13] Press release from the Cassini project team, see http://Saturn.jpl.nasa.gov/multimedia/images/image-details.cfm?imageID=1631